Chemical Engineering Journal 120 (2006) 169–179

Chemical Engineering Journal

www.elsevier.com/locate/cej

Micro-simulated moving bed (μSMB) systems: A numerical study

Hariprasad J. Subramani *, Anjushri S. Kurup

School of Chemical Engineering, Purdue University, IN 47907-2100, USA

Received 8 December 2005; received in revised form 9 April 2006; accepted 10 April 2006

Abstract

Continuous chromatographic separation processes like simulated moving bed (SMB) systems have been employed in petrochemicals, sugar, and more recently, in pharmaceutical industries by virtue of their superior separation efficiency. Miniaturization of chromatography-based analytical techniques (e.g., high performance liquid chromatography, micro-HPLC or μHPLC) has already been successfully demonstrated in the last few years owing to the rapid development in MEMS technology. With such a rapid progress in technology, it is definitely possible to realize the miniaturization of a powerful continuous chromatographic process such as SMB. Micro-SMB (μSMB) systems could not only inherit the merits of μHPLC, but also provide efficient separation of compounds such as isomers and enantiomers that are otherwise very difficult to isolate. In this paper, new simulations of the performance of a μSMB system for the separation of a mixture of phenol and *o*-cresol, using a robust numerical algorithm developed that mimics the dynamic operation of the μSMB system, are presented. A systematic parametric sensitivity analysis that addresses the effects of various process parameters on the performance of the μSMB system is also presented. High purities and yields of both phenol and *o*-cresol is achieved in the μSMB by judicious choice of process parameters.

Keywords: Chromatography; Micro simulated moving bed; Simulation

1. Introduction

With the revolutionary progress in MEMS technology, miniaturized separation techniques have become very popular in the last few years and they offer numerous advantages over conventional separation processes such as reduced chemical consumption, improved mass sensitivity and separation efficiency [1]. Pregnancy and cholesterol test kits available at home nowadays are essentially micro-labs housing sampling, separation, reaction, and detection units [2]. Many of the separation techniques based on chromatography that are employed in chemical, biomedical and environmental sciences have also been successfully miniaturized. For example, miniaturized versions of high performance liquid chromatography (μHPLC) that are either packed micro-columns [1–4] or surface-functionalized micro monoliths [5,6] have already been demonstrated to isolate species at reduced chemical consumption and with better sensitivity.

Besides being ubiquitously employed as an excellent analytical system, HPLC is widely used in preparative and production-scale systems [7,8]. Implementation in production-scale systems necessitates the need for employing continuous chromatographic systems [9]. Simulated moving bed (SMB) [10] and its variant VARICOL® [11,12] are two of the conventional yet powerful continuous chromatographic systems that have been successfully implemented in various industrial applications.

A schematic representation of a SMB system is illustrated in Fig. 1 that consists of a number of packed (with adsorbent particles of diameter d_p) columns of uniform cross-section connected in a circular array, each of length L_{col} and diameter d_{col}. The two incoming streams (the feed, F, and the desorbent/eluent, D) and the two outgoing streams (the raffinate, Ra, and the extract, Ex) divide the system into four sections (zones), namely P, Q, R and S, each of which is comprised of p, q, r and s columns, respectively. The flow rates in the sections P, Q, R and S are designated as Q_P, Q_Q, Q_R and Q_S, respectively, while those of the feed, raffinate, eluent/desorbent and extract are designated as Q_F, Q_{Ra}, Q_D and Q_{Ex}, respectively. However, only four of the above eight flow rates are independent, as the remaining four are determined from the mass balance at points (nodes) A, B, C and D (as shown in Fig. 1). By suitably advancing the inlet and outlet ports, column by column, in the direction of the fluid flow at a pre-set switching time, t_s, the countercurrent movement of the

* Corresponding author.
E-mail address: hsubrama@ecn.purdue.edu (H.J. Subramani).

1385-8947/$ – see front matter © 2006 Elsevier B.V. All rights reserved.
doi:10.1016/j.cej.2006.04.002

Nomenclature

a_i	Langmuir isotherm constant of 'i'th component
b_i	Langmuir isotherm constant of 'i'th component (l/mol)
a_{ij}	quadratic isotherm interaction constant (l/mol)
b_{ij}	quadratic isotherm interaction constant (l/mol)^2
C	liquid phase concentration (mol/l)
C_0	initial liquid phase concentration (mol/l)
D_{ax}	axial diffusivity (cm^2/min)
d_{col}	column diameter (cm)
d_p	particle diameter (cm)
L_{col}	column length (cm)
m_i	dimensionless solid velocity (based on triangle theory)
Pe	Peclet number
P_P	purity of phenol (%)
P_C	purity of *o*-cresol (%)
q	concentration in the solid phase (mol/l)
q^*	concentration at solid phase in equilibrium with mobile phase (mol/l)
Q_F	feed flow rate (ml/min)
Q_i	flow rate in section 'i = P, Q, R, S' (ml/min)
t_s	switching period (min)
U_F	fluid interstitial velocity (cm/min)
V_{col}	column volume (cm^3)
Y_P	yield of phenol (%)
Y_C	yield of *o*-cresol (%)

Greek letters

α	lumped mass transfer coefficient (min^{-1})
α_m	lumped dimensionless mass transfer coefficient
ε	bed porosity
ν	solid to fluid volume ratio
ζ	solid velocity
χ	dimensionless length
θ	dimensionless time

Superscripts and subscripts

D	desorbent or eluent
Ex	extract
F	feed
P, Q, R, S	sections of the SMB
Ra	raffinate

solids is simulated. This switching time is the key parameter, which defines the hypothetical solid velocity ($\zeta \sim L_{col}/t_s$). However, the countercurrent separation of the components could be achieved only by judiciously specifying the internal flow rates in the columns besides the switching time.

An exhaustive literature is available on conventional SMB systems. Theories like McCabe-Thiele method [9], triangle theory [13,14], and standing wave design [15] have also been developed over the years that have become quite popular in the operability design of SMB systems. Researchers have successfully demonstrated using SMB to obtain high purity and yield of

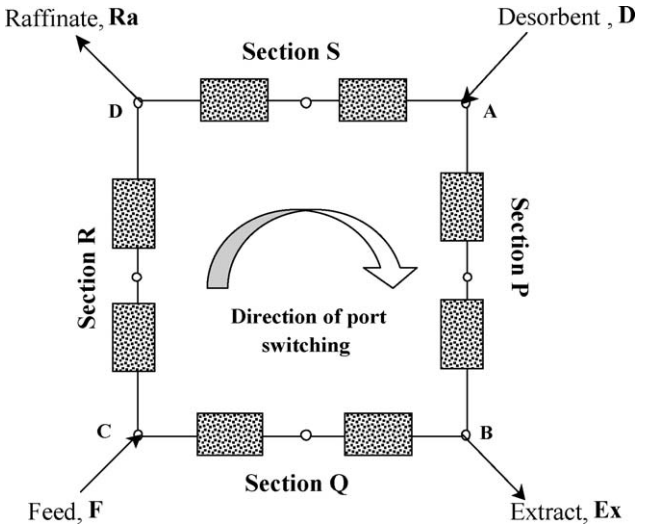

Fig. 1. A schematic representation of a four zone (two columns per zone) SMB system.

species from a variety of mixtures that include aromatics [16], sugars [17–19], and more recently enantiomers [11,12,20–23]. Several researchers have also reported design and optimization methodologies [13–16,18,19,21,24,25] to achieve optimal separation using SMB. Attempts have also been successful in employing SMB as an in situ reactor-separator [26–28].

2. Micro-simulated moving bed (μSMB) system

Enantiomers, which are routinely used in pharmaceuticals, have near unity partition coefficients and are very difficult to isolate. As mentioned earlier, SMB systems have been proven to be highly effective in isolating components like isomers and enantiomers (with partition coefficient → 1) that are difficult to separate via other chromatographic techniques. Not only that these compounds are very expensive but also the adsorbents and eluents/desorbents used in SMB are very costly. Hence, there is always a need for reduction in the volume of columns, con-

Table 1
Operating and adsorption parameters for single column elution in conventional HPLC [30]

L_{col} (mm)	150.0
d_{col} (mm)	3.3
d_p (μm)	7.0
V_i (μl)	550.0
Q_i (ml/min)	1.0
$C_{0,P}$ (mol/l)	0.1
$C_{0,C}$ (mol/l)	0.1
υ (–)	0.49
a_1 (–)	5.4
a_2 (–)	12.48
b_1 (mol/l)$^{-1}$	2.85
b_2 (mol/l)$^{-1}$	7.5
a_{12} (mol/l)$^{-1}$	11.7
a_{21} (mol/l)$^{-1}$	−12.8
b_{12} (mol/l)$^{-2}$	−10.69
b_{21} (mol/l)$^{-2}$	−24.7

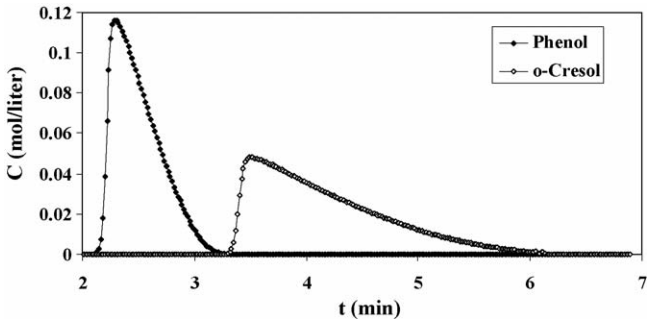

Fig. 2. Simulated concentration elution profile in a conventional HPLC for phenol and *o*-cresol obtained at experimental conditions (cf. Table 1) reported by Jandera et al. [30]. Separon SGX C_{18} microparticles (7 μm) is the packing material and 30% (by volume) of methanol in water is the desorbent.

Table 2
Operating and adsorption parameters for single column elution in μHPLC [4]

L_{col} (mm)	143.0
d_{col} (μm)	320.0
d_p (μm)	5.0
V_i (μl)	5.5
Q_i (μl/min)	5.0
$C_{0,P}$ (mol/l)	0.1
$C_{0,C}$ (mol/l)	0.1
υ (–)	0.44
a_1 (–)	3.87
a_2 (–)	5.52
b_1 (mol/l)$^{-1}$	0.49
b_2 (mol/l)$^{-1}$	2.05

sumption of eluent and yet maintain high purity and yield of product species. Inspired by the recent works on miniaturization of HPLC columns [1–6], an attempt has been made in this paper, to investigate the performance of a micro-SMB (μSMB) system by numerical simulations. Micro-SMB systems, apart from inheriting the various afore-mentioned advantages of the μHPLC columns, can also be very effective in separating compounds that are very difficult to isolate via other separation techniques. Also with a better understanding of the performance of μSMB systems, one can envision the possibility of integrating the μSMB system as a reactor-separator given that conventional SMB has already been demonstrated to efficiently serve as an in situ reactor-separator [26–28].

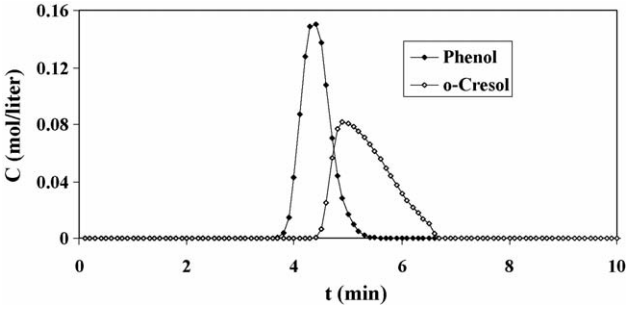

Fig. 3. Simulated concentration elution profile in a μHPLC for phenol and *o*-cresol obtained at experimental conditions (cf. Table 2) reported by Jandera et al. [4]. Separon SGX C_{18} microparticles (5 μm) is the packing material and 50% (by volume) of methanol in water is the desorbent.

Table 3
Reference process parameters for μSMB

L_{col} (mm)	50.0
d_{col} (μm)	320.0
d_p (μm)	5.0
p, q, r, s (column configuration)	1, 2, 2, 1
Q_P (μl/min)	20.0
Q_Q (μl/min)	15.34
Q_R (μl/min)	15.4
Q_S (μl/min)	12.0
$C_{0,P}$ (mol/l)	0.1
$C_{0,C}$ (mol/l)	0.1
υ (–)	0.44
α (min^{-1})	150.0
a_1 (–)	3.87
a_2 (–)	5.52
b_1 (mol/l)$^{-1}$	0.49
b_2 (mol/l)$^{-1}$	2.05

The primary goal of the present study is to systematically study the influence of different process parameters on the performance of the μSMB system. The separation of a binary mixture of phenol and *o*-cresol using 50% (by volume) methanol in water as the eluent over Separon SGX C_{18} microparticles (5 μm) as adsorbent [4] is chosen as the model system in the present study. Phenol is the weakly adsorbed species and hence collected from the raffinate stream, while *o*-cresol is the strongly adsorbed one which is collected from the extract stream. In what follows, the

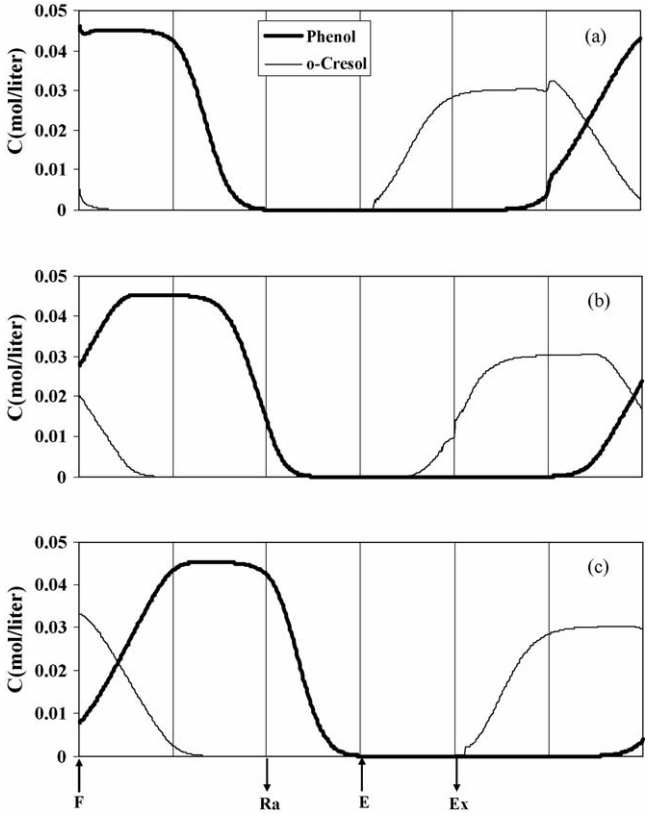

Fig. 4. Simulated concentration profiles in a μSMB system for phenol and *o*-cresol at cyclic steady state: (a) start; (b) middle; and (c) end of the switching period (t_s = 0.52 min). The process parameters are listed in Table 3.

development and validation of the numerical algorithm for the μSMB system is discussed. The parametric sensitivity of various process parameters such as the switching time (t_s), number of columns (p, q, r, s) in each section (P, Q, R, S) of the μSMB, the different section flow rates (Q_P, Q_Q, Q_R, Q_S) on the performance of the μSMB system is then discussed. Finally, the concluding remarks and the outlook of future research are presented.

3. Numerical model

A mathematical model that has been proven to mimic conventional SMB systems [16,18,19] very well is employed in the present study to capture the dynamic behavior of the μSMB system. The differential transient mass balance equations along with the boundary conditions are as follows:

$$\frac{\partial C_{i,k}}{\partial \theta} + \upsilon \frac{\partial q_{i,k}}{\partial \theta} = \frac{\psi_k}{Pe_k} \frac{\partial^2 C_{i,k}}{\partial \chi^2} - \psi_k \frac{\partial C_{i,k}}{\partial \chi} \tag{1}$$

$$\frac{\partial q_{i,k}}{\partial \theta} = \alpha_m (q^*_{i,k} - q_{i,k}) \tag{2}$$

where $C_{i,k}$ is the concentration of the 'i'th species in the liquid in the ''k'th column, $q^*_{i,k}$ the concentration in the solid phase in equilibrium with that in the liquid, $q_{i,k}$ the concentration in the solid, $\chi = z/L_{col}$ the dimensionless length, $\upsilon = (1-\varepsilon)/\varepsilon$ the ratio of volumes of solid to liquid phases, ε the bed porosity, $\alpha_m = t_s\alpha$ the dimensionless mass transfer coefficient and $\theta = t/t_s$

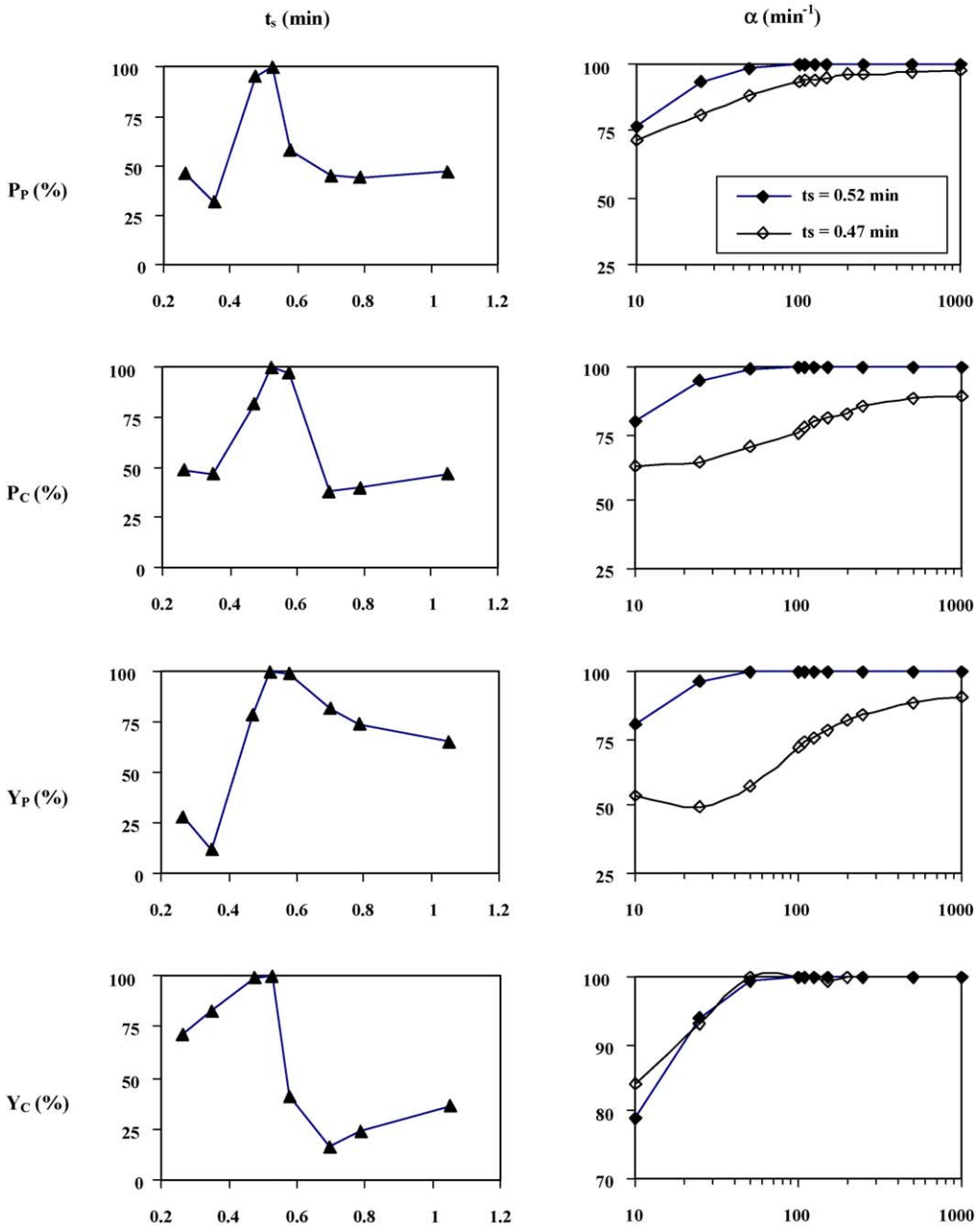

Fig. 5. Effects of switching time (t_s) and mass transfer coefficient (α) on the performance of μSMB system. Reference parameters are listed in Table 3.

is the dimensionless time. The other dimensionless parameters in the above equations are the ratio of liquid to solid velocities ($\psi_k = U_{F_z} t_s / L_{col}$) and Peclet number ($Pe_k = U_{F_k} L_{col} / D_{ax_k}$).

As the column diameter is decreased, the adsorption isotherm parameters of the different species, though being thermodynamic properties, change due to differences in packing density and inaccurate measurements of extra-column volumes [4]. Hence, adsorption isotherms measured using conventional HPLC columns may not hold good for μSMB system. Jandera et al. [3,4,29] and Jandera and Komers [30] reported a series of systematic measurements of isotherms using various conventional and packed μHPLC columns. In the present study, either a competitive Langmuir isotherm (Eq. (3)) obtained from a μHPLC column [4] or a competitive quadratic isotherm (Eq. (4)) [30] (for the validation of the algorithm) reported by Jandera et al. is used to describe the multi-component adsorption equilibria.

$$q^*_{i,k} = \frac{a_i C_{ik}}{1 + \sum_{j=1}^{2} b_j C_{jk}} \tag{3}$$

$$q^*_{i,k} = \frac{a_i C_{ik} + a_{ip} C_{ik} C_{pk}}{1 + \sum_{j=1}^{2} b_j C_{jk} + b_{ip} C_{ik} C_{pk}}; \quad (p \neq i) \tag{4}$$

The boundary conditions are:

$$C^{in}_{i,\chi} = C_{i,k}(0,\ \theta) - \frac{1}{Pe_k} \frac{\partial C_{i,k}}{\partial \chi} \tag{5}$$

$$\frac{\partial C_{i,k}}{\partial \chi}(1,\ \theta) = 0 \tag{6}$$

The initial conditions are:

$$C_{i,k}(\chi,\ 0) = C^0_{i,k}(\chi) \quad \text{and} \quad q_{i,k}(\chi,\ 0) = q^0_{i,k}(\chi) \tag{7}$$

The mass balance at the node is then,

$$C^{in}_{i,k} = C_{i,k-1}(1,\ \theta) \tag{8}$$

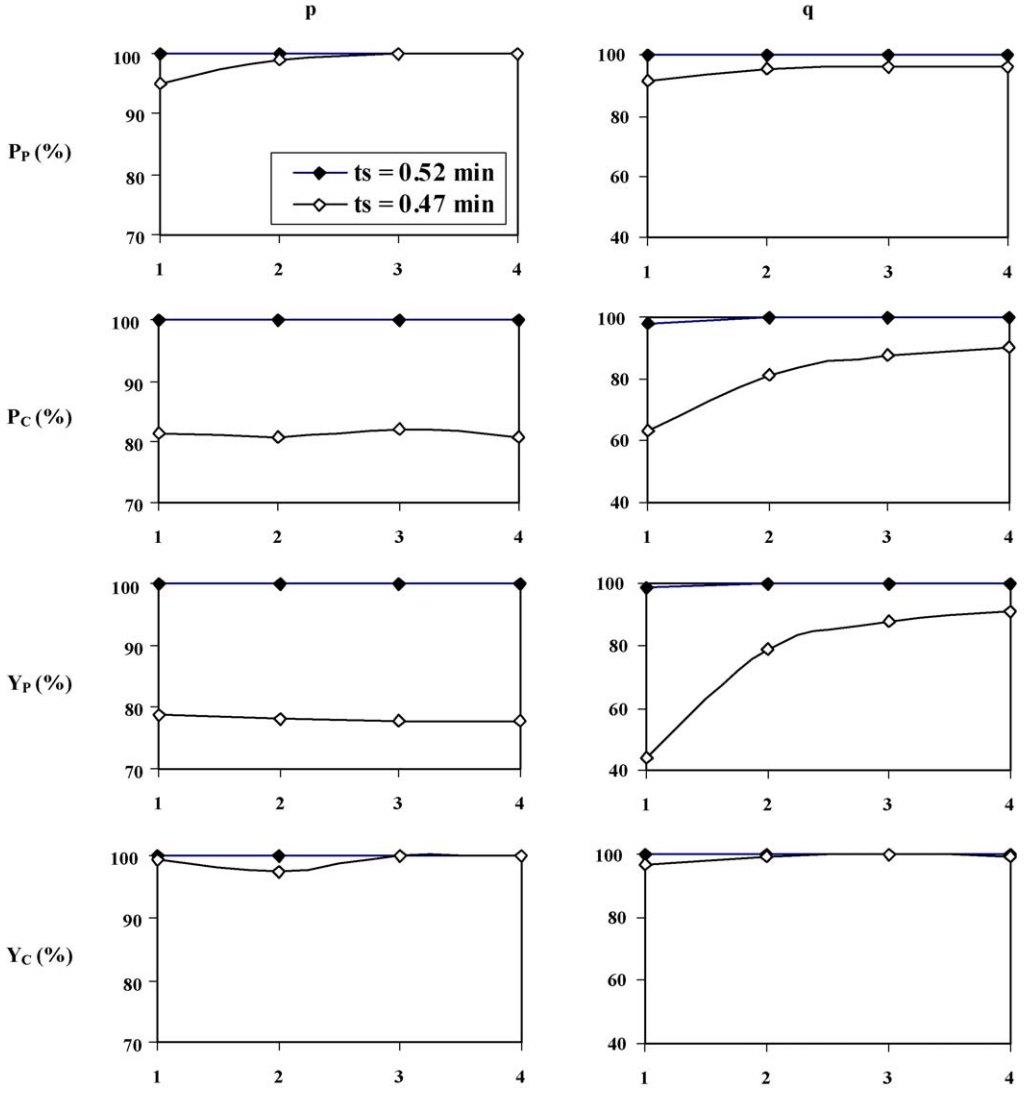

Fig. 6. Effects of number of columns (p and q) in sections P and Q, respectively, on the performance of μSMB system. Reference parameters are listed in Table 3.

except if the column follows feed or desorbent port in which case,

$$C_{i,k}^{\text{in}} = \frac{[Q_{\text{F}}C_{i,\text{F}} + Q_{\text{Q}}C_{i,k-1}(1,\,\theta)]}{Q_{\text{R}}} \quad \text{and}$$

$$C_{i,k}^{\text{in}} = \frac{Q_{\text{S}}C_{i,k-1}(1,\,\theta)}{Q_{\text{P}}}, \tag{9}$$

respectively.

The resulting system of PDEs are discretized in space using the finite difference approximations to convert them into a system of coupled ODE-IVPs (Method of Lines) [22,27,28]. Each column length is spatially discretized using 100 grid points. These stiff initial value ODEs were solved using a robust algorithm developed in FORTRAN90 along with the subroutine, DIVPAG (based on Gear's method), in the IMSL library. Since a periodic switching is imposed on the system, the μSMB system operates under transient conditions. However, a cyclic (periodic) steady state with a period equal to the global switching time is eventually reached after several switchings. For the system studied in this paper, a periodic steady state is attained after about 150 switching cycles. High mass transfer rates are assumed and the Peclet number is calculated using the commonly used correlation [31]. The purities (%) of phenol and *o*-cresol are designated as P_{P} and P_{C}, respectively, while their yields (%) are denoted by Y_{P} and Y_{C}, respectively. The definitions of the purity and yield of the two species, respectively, are as follows:

$$P_{\text{P}} = \frac{C_{\text{P}}^{\text{Ra}}}{C_{\text{P}}^{\text{Ra}} + C_{\text{C}}^{\text{Ra}}} \times 100 \tag{10}$$

$$P_{\text{C}} = \frac{C_{\text{C}}^{\text{Ex}}}{C_{\text{P}}^{\text{Ex}} + C_{\text{C}}^{\text{Ex}}} \times 100 \tag{11}$$

$$Y_{\text{P}} = \frac{Q_{\text{Ra}}C_{\text{P}}^{\text{Ra}}}{Q_{\text{F}}C_{0,\text{P}}} \times 100 \tag{12}$$

$$Y_{\text{C}} = \frac{Q_{\text{Ex}}C_{\text{C}}^{\text{Ex}}}{Q_{\text{F}}C_{0,\text{C}}} \times 100 \tag{13}$$

The algorithm developed is benchmarked by first simulating the single-column elution curves of phenol and *o*-cresol in a HPLC column (3.3 mm) at the experimental process parameters (cf. Table 1) reported by Jandera and Komers [30]. Fig. 2 clearly elucidates that the simulated elution curves are in excel-

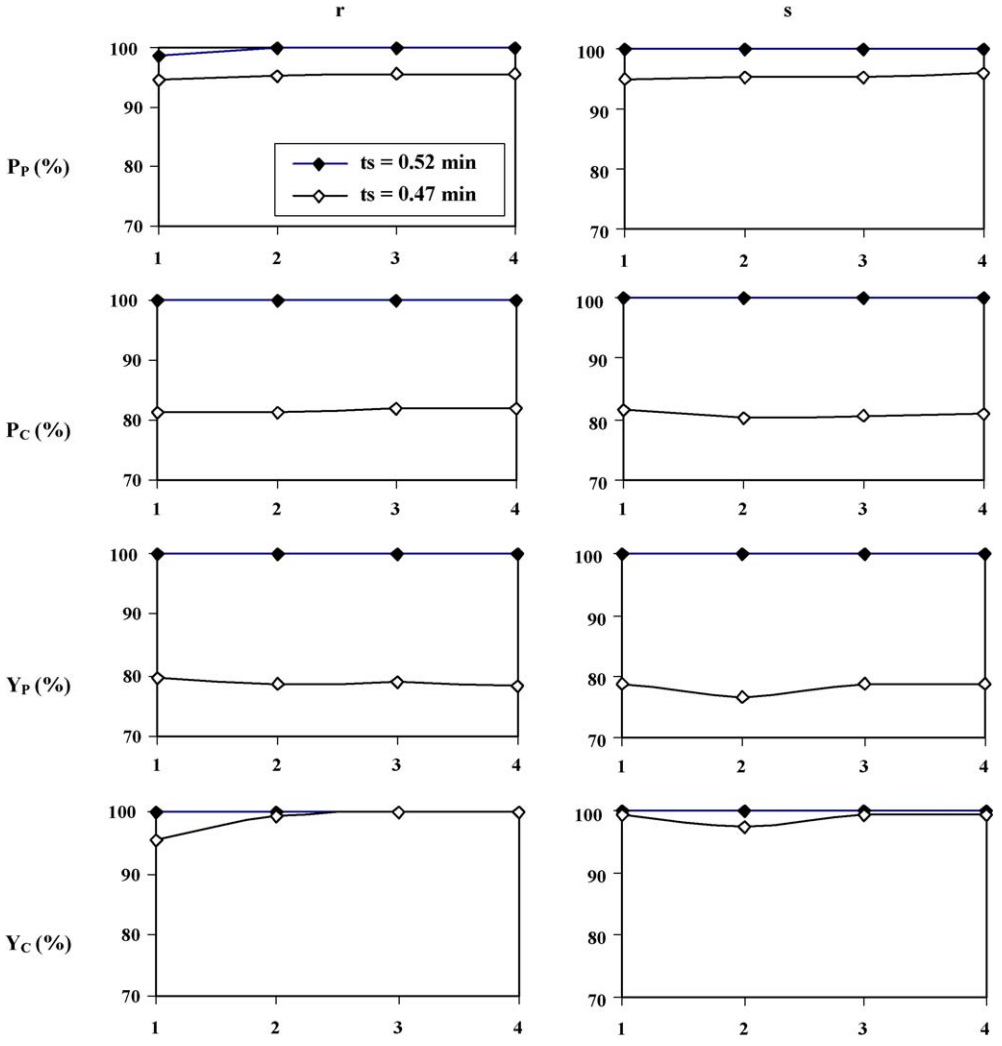

Fig. 7. Effects of number of columns (r and s) in sections R and S, respectively, on the performance of μSMB system. Reference parameters are listed in Table 3.

lent agreement with the experimental curves [30]. Jandera et al. [4] also reported adsorption isotherms of phenol and *o*-cresol obtained from a micro-HPLC column (320 μm). Though the authors reported the experimental process parameters for the single column elution measurements (cf. Table 2), they did not report the elution curve which could have been beneficial to benchmark the present algorithm. For completeness, the simulated elution curves in a μHPLC column at the experimental conditions listed in Table 2 [4] are illustrated in Fig. 3. Clearly, the separation (Fig. 3) under the experimental conditions is not as efficient as that from the conventional HPLC column (Fig. 2).

4. Results and discussion

Mazzotti et al. [13,14] have shown through the now-so-popular triangle theory that complete separation is possible if the dimensionless solid velocity m_i (i = P, Q, R, S) in the different sections of SMB satisfies a set of inequalities.

$$m_i = \frac{Q_i t_s - V_{col}\varepsilon}{V_{col}(1-\varepsilon)} \tag{14}$$

Following the triangle theory [13,14], a series of simulations are performed to find out a set of process parameters for the μSMB system where complete separation of phenol and *o*-cresol is achieved. A switching period (t_s) of 0.52 min for the μSMB system (L_{col} = 5 cm, d_{col} = 320 μm, d_p = 5 μm, υ = 0.44) that consisted of a column configuration of 1-2-2-1 in the P, Q, R, and S sections, respectively, and other judicious choice of process parameters (cf. Table 3) satisfies the constraints of the triangle theory for the competitive Langmuir isotherm [4] which aptly describes the distribution of phenol and *o*-cresol in the solid and liquid phases. Fig. 4 elucidates the simulated concentration profiles of phenol and *o*-cresol (under the afore-mentioned conditions; also as listed in Table 3) in the four different sections of the μSMB system at the beginning (see Fig. 4(a)), middle (Fig. 4(b)) and end of the switching period (Fig. 4(c)) after cyclic steady state is attained. Fig. 4 clearly shows that complete sep-

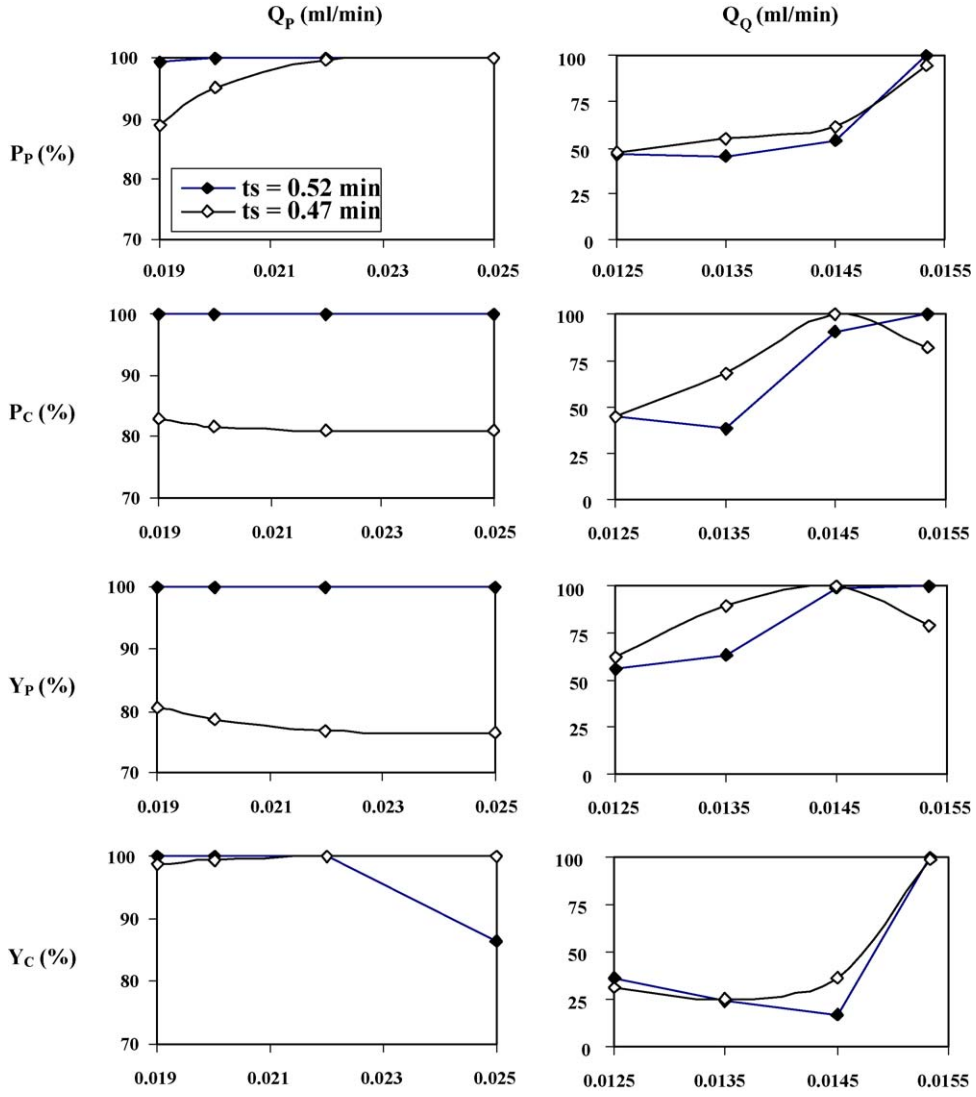

Fig. 8. Effects of flow rates in sections P and Q, respectively, on the performance of μSMB system. Reference parameters are listed in Table 3.

aration of the two species (100% purity and yield of phenol and *o*-cresol, respectively), is achieved. Under the flow conditions as given in Fig. 4, achieving the desired pressure drop for flow through micro-columns is of prime importance. However, using the classical Ergun's equation [32], the pressure drop between the ends of the columns of the μSMB system is determined to be of the order of 1 atm, which can be readily achieved by the instrumentation described by Jandera et al. [3,4,29] and Jandera and Komers [30].

The variations in performance of the μSMB with changes in switching period (t_s) and mass transfer coefficient (α) at fixed values of all other process parameters (cf. Table 3) are elucidated in Fig. 5. Clearly, there is an optimal value of t_s at which both phenol and *o*-cresol are separated with 100% purity and yield, respectively. Under the reference conditions, complete separation is achieved with a switching period of 0.52 min. However, when t_s is slightly changed to 0.47 min, both the species are not obtained at 100% purity. As expected, as the mass transfer coefficient (α) is increased, complete separation is achieved when $t_s = 0.52$ min. Also, it is evident from Fig. 5 that even at high α, when $t_s = 0.47$ min, complete separation is not achieved.

Figs. 6 and 7 illustrate the effect of the number of columns in the different sections on the performance of μSMB system at two different t_s while holding the other process parameters constant (cf. Table 3). When $t_s = 0.52$ min, the number of columns in all the sections (P, Q, R and S) hardly affects the system performance and always complete separation is achieved. However, when section R (feed section) consists of only one column (with other parameters fixed) at $t_s = 0.52$ min, the solid volume in the feed section is not enough to completely adsorb *o*-cresol and hence the purity of phenol is affected (cf. Fig. 7). Also it is evident from Figs. 6 and 7 that the system performance is severely affected by the change in the number of columns when $t_s = 0.47$ min. Both components are not obtained at 100% purity and yield in this case. While the purity and yield of one of the components is improved, those of the other component are diminished, which implies that there is a complex interplay of the various process parameters on the performance of the μSMB system.

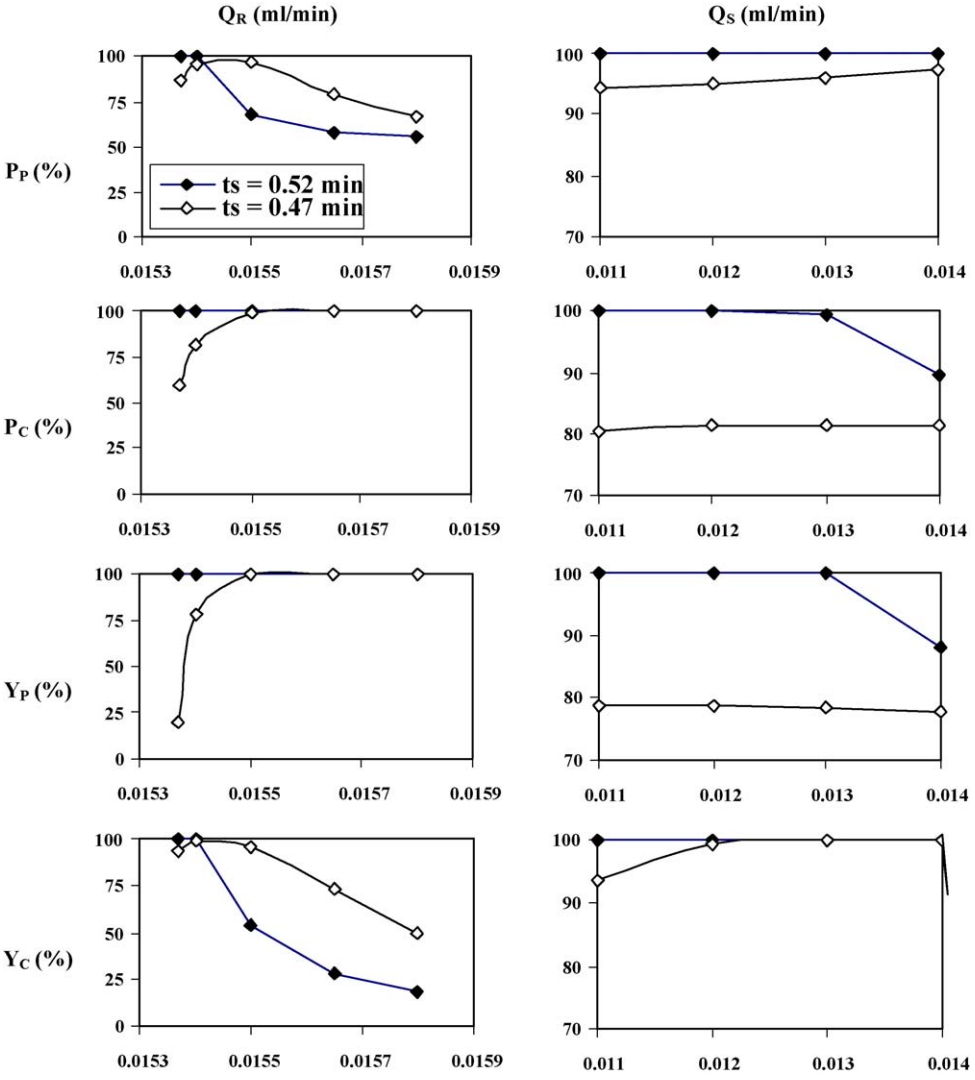

Fig. 9. Effects of flow rates in sections R and S, respectively, on the performance of μSMB system. Reference parameters are listed in Table 3.

The change in the system performance with variations in the different section flow rates (at constant values of other parameters listed in Table 3) at two different t_s is explicated in Figs. 8 and 9. Again, the system performance is mostly superior when $t_s = 0.52$ min compared to that when $t_s = 0.47$ min. The variations in the internal flow rates in sections P and S do not affect the purity and yield of both species significantly when $t_s = 0.52$ min. Complete separation is achieved for a wide range of Q_P and Q_S at $t_s = 0.52$ min. However, the variations in the flow rates Q_Q and Q_R significantly affect the purity and yield of the two components even when $t_s = 0.52$ min. Low (high) values of Q_Q (Q_R), holding other parameters constant, causes (implies) an increase in the feed flow rate (Q_F) that can be too high to be handled by the volume of adsorbent in section R thereby hampering the purity (as low as 50%) and yield (as low as 20%) of both components (cf. Figs. 8 and 9). However, it is evident from Fig. 9 that when $t_s = 0.47$ min, as Q_R is increased, the system performance is superior compared to that when $t_s = 0.52$ min. This could be attributed to the increase in solid phase velocity ($\zeta \sim L_{col}/t_s = 10.64$ cm/min) due to the small t_s (at high $t_s = 0.52$ min, $\zeta \sim 9.62$ cm/min) which compensates for the increase in feed flow rate (Q_F).

It is also imperative to find out if there is any room for reduction in the volume of the columns (by decreasing L_{col}) and still achieve complete separation of the product species. Also it is essential to see if complete separation can be achieved with changes in the feed concentration. Fig. 10 elucidates the effect of the variations in α at two different L_{col} (at other constant parameters listed in Table 3) on the purity and yield of phenol and *o*-cresol. When L_{col} is 3 cm, t_s is set to be 0.31 min so that the solid phase velocity (ζ) is still maintained at 9.62 cm/min (which is the case when $L_{col} = 5$ cm and $t_s = 0.52$ min). This ensures that

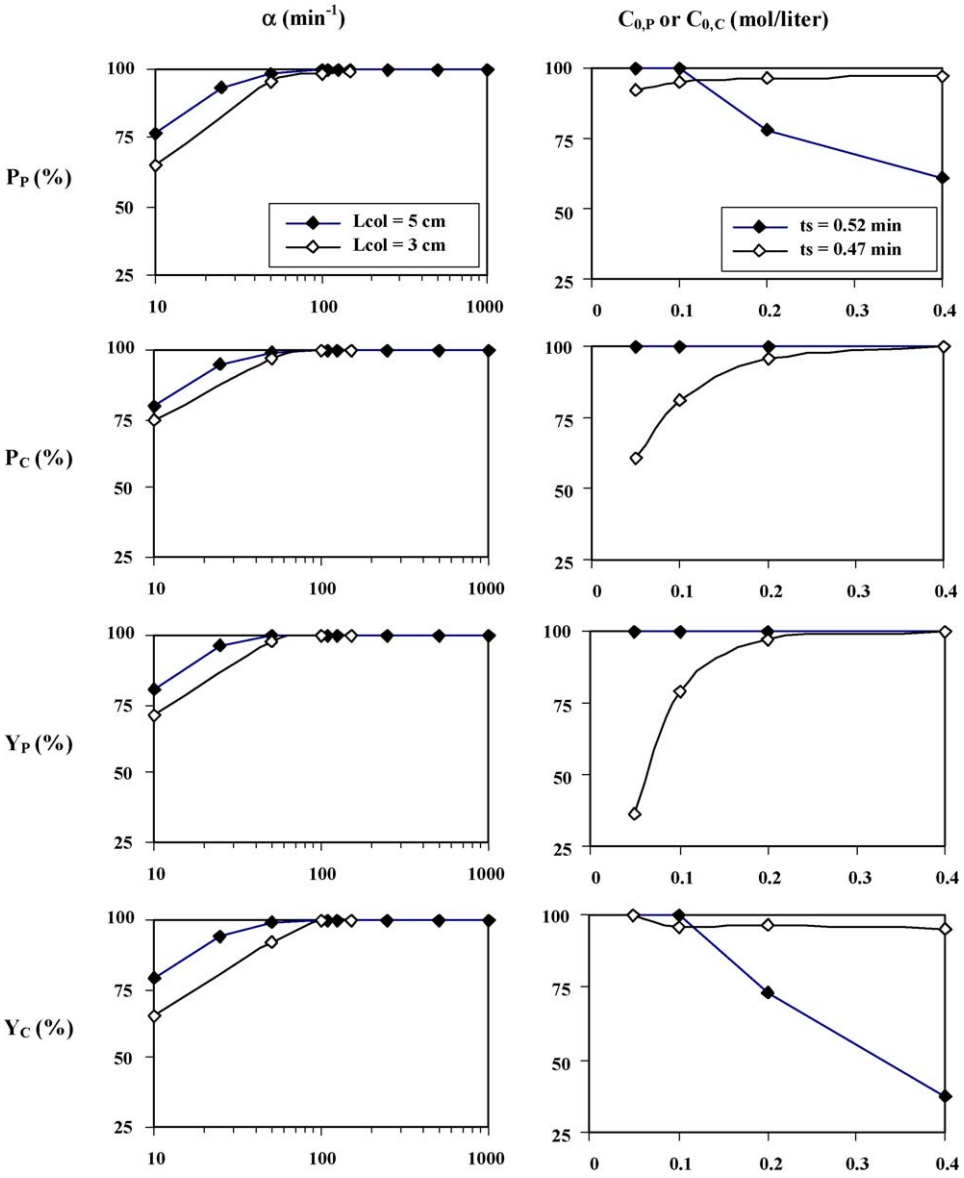

Fig. 10. Effects of α (for different L_{col}) and feed concentration (C_0) on the performance of μSMB system. For each L_{col}, t_s is chosen such that $\zeta = 9.62$ cm/min. Other reference parameters are listed in Table 3.

at the reference values of all other parameters, the μSMB system provides complete separation of the components (cf. Fig. 10). However, it is worth noting that the decrease in length of the column is also subjected to the experimental constraints as the operation of μSMB involves complicated instrumentation. Also shown in Fig. 10 is the effect of changes in feed concentration (C_0) on the system performance. It is evident from Fig. 10 that as the feed concentration of both the components is increased (by equal amounts), the purity and yield of one of the species always gets diminished. This reiterates the fact that the performance of the μSMB system is strongly influenced by the complex interplay of the various process parameters.

5. Conclusions

Numerical simulations presented in this paper capture the dynamic behavior of a novel μSMB system for the separation of a model system (viz., a mixture of phenol and *o*-cresol). Judicious choice of process parameters based on triangle theory [13,14] provides complete separation of phenol and *o*-cresol. However, the performance of the μSMB system is affected in a complex manner by various process parameters. Slight changes in the process parameters result in the decrease in purity and yield of at least one of the species in some cases and in the worst scenario, affects both the species. A systematic and comprehensive optimization study needs to be performed to achieve optimal operation of the μSMB system. Experimental validation is yet another and important logical step.

Drawing inspiration from the MEMS community, where researchers aim at developing integrated micro-devices to enhance the throughput, the integration of the μSMB systems could be envisaged as an option. Also, the μSMB system has the potential to serve as an in situ reactor-separator (like conventional reactive SMB systems [26–28]), which could open new avenues for the micro-reactor research community.

Acknowledgements

We sincerely thank the anonymous referees for their comments and suggestions.

References

[1] M. Szumski, B. Buszewski, State of the art in miniaturized separation techniques, Crit. Rev. Anal. Chem. 32 (2002) 1–46.
[2] F.E. Regnier, B. He, S. Lin, J. Busse, Chromatography and electrophoresis on chips: critical elements of future integrated, microfluidic analytical systems for life science, Trends Biotechnol. 17 (1999) 101–106.
[3] P. Jandera, S. Buncekova, J. Planeta, Separation of isomeric naphthalenesulphonic acids by micro high-performance liquid chromatography with mobile phases containing cyclodextrin, J. Chromatogr. A 871 (2000) 139–152.
[4] P. Jandera, S. Buncekova, K. Mihlbachler, G. Guiochon, V. Backovska, J. Planeta, Fitting adsorption isotherms to the distribution data obtained using packed micro-columns for high-performance liquid chromatography, J. Chromatogr. A 925 (2001) 19–29.
[5] D.S. Reichmuth, T.J. Shepodd, B.J. Kirby, Microchip HPLC of peptides and proteins, Anal. Chem. 77 (2005) 2997–3000.
[6] B.H. Lapizco-Encinas, N.G. Pinto, Performance characteristics of novel open parallel plate separator, Sep. Sci. Technol. 37 (2002) 2745–2762.
[7] G. Ganetsos, P.E. Barker (Eds.), Preparative and Production Scale Chromatography, Marcel Dekker, New York, 1993.
[8] G. Guiochon, S.G. Shirazi, A.M. Katti, Fundamentals of Preparative and Nonlinear Chromatography, Academic Press, Boston, 1994.
[9] D.M. Ruthven, C.B. Ching, Countercurrent and simulated countercurrent adsorption separation processes, Chem. Eng. Sci. 44 (1989) 1011–1038.
[10] D.B. Broughton, C.G. Gerhold, Continuous sorption process employing fixed bed of sorbent and moving inlets and outlets, US Patent 2985589 (1961).
[11] O. Ludemann-Hombourger, R.M. Nicoud, M. Bailly, The "VARICOL" process: a new multicolumn continuous chromatographic process for chiral separation, Sep. Sci. Technol. 35 (2000) 1829–1862.
[12] O. Ludemann-Hombourger, G. Pigorini, R.M. Nicoud, D.S. Ross, G. Terfloth, Application of the VARICOL process to the separation of the isomers of the SB-553261 racemate, J. Chromatogr. A 947 (2002) 59–68.
[13] M. Mazzotti, G. Storti, M. Morbidelli, Robust design of countercurrent adsorption separation: 3. Nonstoichiometric systems, AIChE J. 42 (1996) 2784–2796.
[14] M. Mazzotti, G. Storti, M. Morbidelli, Optimal peration of simulated moving bed units for nonlinear chromatographic separations, J. Chromatogr. A 769 (1997) 3–24.
[15] Z. Ma, N.-H.L. Wang, Standing wave analysis of SMB chromatography: linear systems, AIChE J. 43 (1997) 2488–2508.
[16] A.S. Kurup, K. Hidajat, A.K. Ray, Optimal operation of an industrial-scale Parex process for the recovery of *p*-xylene from a mixture of C_8 aromatics, Ind. Eng. Chem. Res. 44 (2005) 5703–5714.
[17] K. Hashimoto, S. Adachi, H. Noujima, H. Maruyama, Models for separation of glucose–fructose mixture using a simulated moving bed adsorber, J. Chem. Eng. Jpn. 16 (1983) 400–406.
[18] D.C.S. Azevedo, A.E. Rodrigues, Fructose–glucose separation in a SMB pilot unit: modelling, simulation, design and operation, AIChE J. 47 (2001) 2042–2051.
[19] H.J. Subramani, K. Hidajat, A.K. Ray, Optimization of simulated moving bed and Varicol processes for glucose–fructose separation, Chem. Eng. Res. Des. 81 (2003) 549–567.
[20] D.C.S. Azevedo, L.S. Pais, A.E. Rodrigues, Enantiomers separation by simulated moving bed chromatography: non-instantaneous equilibrium at the solid–fluid interface, J. Chromatogr. A 865 (1999) 187–200.
[21] J. Strube, A. Jupke, A. Epping, H. Schmidt-Traub, M. Schulte, R. Devant, Design, optimization and operation of SMB chromatography in the production of enantiometrically pure pharmaceuticals, Chirality 11 (1999) 440–450.
[22] Z. Zhang, K. Hidajat, A.K. Ray, M. Morbidelli, Multi-objective optimization of simulated moving bed system and Varicol process for chiral separation, AIChE J. 4 (2002) 2800–2816.
[23] F. Wongso, K. Hidajat, A.K. Ray, Optimal operating mode for enantioseparation of SB-553261 racemate based on SMB technology, Biotechnol. Bioeng. 87 (2004) 704–722.
[24] C. Heurer, E. Kusters, T. Plattner, A. Seidel-Morgenstern, Design of the simulated moving bed process based on adsorption isotherm measurements using a perturbation method, J. Chromatogr. A 827 (1998) 175–191.
[25] G. Dunnebier, K.U. Klatt, Optimal operation of simulated moving bed chromatographic processes, Comput. Chem. Eng. 23 (1999) S195–S198.
[26] H.J. Subramani, K. Hidajat, A.K. Ray, Optimization of reactive SMB and Varicol systems, Comput. Chem. Eng. 27 (2003) 1883–1901.
[27] W. Yu, K. Hidajat, A.K. Ray, Modeling, simulation and experimental study of a simulated moving bed reactor for the synthe-

sis of methyl acetate ester, Ind. Eng. Chem. Res. 42 (2003) 6743–6754.
[28] A.S. Kurup, H.J. Subramani, K. Hidajat, A.K. Ray, Optimal design and operation of SMB bioreactor for sucrose inversion, Chem. Eng. J. 108 (2005) 19–33.
[29] P. Jandera, Z. Posvec, P. Vraspir, Mobile phase effects on single-component and competitive adsorption isotherms in reversed-phase systems, J. Chromatogr. A 734 (1996) 125–136.
[30] P. Jandera, D. Komers, Fitting competitive adsorption isotherms to the experimental distribution data in reversed-phase systems, J. Chromatogr. A 762 (1997) 3–13.
[31] S.F. Chung, C.Y. Wen, Longitudinal dispersion of liquid flowing through fixed and fluidized beds, AIChE J. 14 (1968) 857–866.
[32] R.B. Bird, W.E. Stewart, E.N. Lightfoot, Transport Phenomena, John Wiley & Sons, New York, 1960.